



## Kaolin intercalated by urea. Ceramic applications



S. Seifi<sup>b,c</sup>, M.T. Diatta-Dieme<sup>a,b</sup>, P. Blanchart<sup>b,\*</sup>, G.L. Lecomte-Nana<sup>b</sup>, D. Kobor<sup>a</sup>, S. Petit<sup>c</sup>

<sup>a</sup> Laboratoire de Chimie et Physique des Matériaux (LCPM), Université Assane SECK de Ziguinchor, BP 523, Senegal

<sup>b</sup> Laboratoire Science des Procédés Céramiques et Traitements de Surface, SPCTS, Centre Européen de la Céramique, 12 Rue Atlantis, 87068 Limoges, France

<sup>c</sup> Université de Poitiers, CNRS-UMR 7285 IC2MP, HydrASA, 4 rue Michel Brunet, 86073 Poitiers Cedex 9, France

### HIGHLIGHTS

- The intercalation degree of kaolinite by urea is 69% when aqueous mixing is used.
- Bonds are formed between inner-surface hydroxyls of kaolinite and NH groups of urea.
- Intercalation increases the densification rate and reduces the sintering temperature.
- Intercalated kaolinite behaves similarly to intensively grounded kaolinite.
- A high intercalation degree of kaolin can be attained in industrial processes.

### ARTICLE INFO

#### Article history:

Received 2 September 2015

Received in revised form 2 March 2016

Accepted 18 March 2016

Available online 24 March 2016

#### Keywords:

Kaolinite

Intercalation

Urea

Silicate ceramic

Sintering

### ABSTRACT

Kaolinite–urea complexes were prepared with kaolinite from KGa-1 kaolin by two techniques, mixing and ball-milling at room temperature in water. The intercalation degree was found to be 72% and 69% respectively. Urea-intercalated kaolinite has potential applications in industry, since it change most of the chemical and thermal behaviors. Particularly, ion intercalation into kaolinite structure changes the amount of reactive acidic and basic sites on the internal and external surfaces. In this study XRD patterns and infrared spectroscopy of kaolinite–urea complexes confirm the intercalation of urea into kaolinite by the expansion of the basal spacing of kaolinite from 0.715 nm to 1.069 nm. The expansion of kaolinite is due to entering urea into interlayers that confirms the occurrence of hydrogen bonding between urea and kaolinite. Thermal analyses (TG, DSC and thermogravimetry) evidence changes in transformation temperatures of intercalated kaolinite. The sintering densification is shifted to lower temperature and kaolinite–urea complexes can be used in new ceramics for building with lower CO<sub>2</sub> specific emission.

© 2016 Elsevier Ltd. All rights reserved.

## 1. Introduction

Industries are major users of clays since it use about 70 wt% of commercial clays. Clay properties of interest in the silicate ceramics industry are plasticity, molding ability, detailed chemical and mineralogical compositions, refractoriness, surface interaction with liquids, thermal and sintering behaviors, and color. They have several applications in construction and in manufacturing, and are also used in the calcined form as fillers (chamotte). As clays are fundamental raw materials for all ceramic compositions, many studies were devoted to improving the role of clays in thermal transformations leading to silicate ceramics having better properties but at a lower cost.

In all countries, considerable amounts of silicate ceramics containing clays are sintered between 900 °C and 1400 °C, in large scale industrial processes. It requires significant amounts of energy and causes significant CO<sub>2</sub> emissions of about 0.25 kg of CO<sub>2</sub> per kg of final product. In particular, the total annual emission of the French bricks and tiles industry is about 1.2 million tons of CO<sub>2</sub> [1,2]. One way to limit emissions is to lower the sintering temperatures, which can be obtained by modifying the behavior with temperature of clays used in compositions, including kaolinite.

In kaolinite mineral, layers are bounded by reactive hydrogen bonds [3–6] and are not easily delaminated [7]. Kaolinite properties can be improved by mechanochemical activation and by intercalation, since they change the surface area, ion-exchange capacity, crystal structure, crystallinity degree and rate of solubility [8,9]. Kaolinite intercalation is due to surfaces interaction with organic molecules and is known for decades [10,11]. Actual researches

\* Corresponding author.

E-mail address: [philippe.blanchart@unilim.fr](mailto:philippe.blanchart@unilim.fr) (P. Blanchart).

are mostly in polymers nano-composites and in inorganic materials. The thermal behavior is also studied since a heating treatment of intercalated kaolinite is necessary for ceramic applications [12]. Different intercalated systems have been reported by many authors but one of the most studied systems is the intercalation of a synthetic polymer, such as kaolinite–potassium acetate [13], kaolinite–formamide [14,15], or kaolinite–urea [9]. In general, methods for the preparation of kaolinite–organic complexes include pressurization, pyrogenation, or mixing of a liquid media [16]. However in industrial processes it is critical to use a low cost and simple method [17], and it has been demonstrated that the mixing of an aqueous suspension is very convenient [18].

In this study, the proposed method is the intercalation of kaolinite by urea, since it is abundantly available at low cost, while having a low environmental impact during its production. With urea, kaolinite can attain a high degree of intercalation with a significantly increased interlayer space. With increasing temperature, the kaolinite–urea complex undergoes very specific structural transformations, which differ from those of a non-intercalated kaolinite. In particular, it leads to a process of dehydroxylation at lower temperature (down to  $\sim 350^\circ\text{C}$  instead of  $\sim 550^\circ\text{C}$ ). After dehydroxylation, intercalated kaolinite becomes a more reactive component, with lower temperatures of structural and microstructural transformations inherent in the formation of silicate ceramics. However, the exact role of urea in these changes is not yet established.

In this work, we demonstrate that simple intercalation method can be used with a representative kaolinite, which is the most frequent material in silicate ceramic industries. We study in details the role of the intercalation process on the thermal and structural transformations, and on the sintering behavior up to  $1300^\circ\text{C}$ . We also study how intercalation of kaolinite is able to reduce the firing temperature of a kaolinite containing composition used in industrial silicate ceramics.

## 2. Materials and methods

The reference Kga-1b kaolin is supplied by the Mineralogical Society. Chemical and mineralogical compositions are reported in Table 1 [19]. The Kga-1b kaolin contains 95 wt% of kaolinite, associated with minor phases such as quartz, hematite and gibbsite. Kga-1b kaolin was used as received and sieved at  $63\ \mu\text{m}$ .

Urea used for this experiment is from VWR. Urea formula is  $\text{CO}(\text{NH}_2)_2$  with a Molar Mass of  $60.06\ (\text{g/mol})$ . Solubility of urea in water is high, about  $105\ \text{g}/100\ \text{mL}$  at  $20^\circ\text{C}$ .

For sample preparation, two intercalation methods were carried out with kaolinite. Firstly we added  $3\ \text{g}$  of kaolinite into  $7\ \text{mol/L}$  urea aqueous solution at  $20^\circ\text{C}$  by stirring during  $48\ \text{h}$ . To separate the excess solution, solid was removed by centrifugation and dried at  $75^\circ\text{C}$  for  $24\ \text{h}$ . A second method is mechanochemical intercalation by mixing  $5\ \text{g}$  of kaolinite with the same aqueous urea solution, but grounded by ball milling during  $1\ \text{h}$  (porcelain jar and balls). The mixture is subsequently centrifuged and dried at  $75^\circ\text{C}$  for  $24\ \text{h}$ .

Thermal transformation and sintering up to  $1300^\circ\text{C}$  were studied with the initial Kga-1b kaolin and with the intercalated Kga-1b kaolin. Additional experiments were performed with a ceramic composition containing mostly the Kga-1b kaolin. The composition is a representative triaxial mixture containing Kga-1b kaolin (50 wt%), fine quartz (25 wt%) and alkaline feldspar (25 wt%). Whereas the considerable spread of compositions for silicate ceramics, this simple mixture is representative of industrial ceramics for floor tiles, sanitary and building materials [20]. Samples were prepared by wet ball milling during  $2\ \text{h}$ , drying the mixture at  $80^\circ\text{C}$ , granulating at  $500\ \mu\text{m}$  through a sieve and pressing in a metallic mold to form small barrels for sintering experiments. The objective is to validate the ceramic application of intercalated kaolinite, using similar processes than that of industries.

Characterizations of all samples by X-ray diffraction (XRD) were carried out with a Philips X'Pert type diffractometer equipped with a  $r = 240\ \text{mm}$  goniometer. We used Cu K $\alpha$  radiation ( $K\alpha = 1.541874\ \text{\AA}$ ) operating at  $40\ \text{kV}$  and  $40\ \text{mA}$ . Scanning rate was  $2^\circ/\text{min}$  in the  $2\theta$  range of  $2\text{--}65^\circ$  for powders and  $2\text{--}35^\circ$  for oriented preparations.

Thermal analyses were carried out with a thermo balance TG–DSC SETARAM (SetSys evolution) under air atmosphere at  $10^\circ\text{C}/\text{min}$  heating rate and  $20^\circ\text{C}/\text{min}$  cooling rate. Alumina as reference material and platinum crucibles were used for the experiments.

FTIR analyses were with a Spectrometer Nicolet 760 Magna IR, with the Nicolet's OMNIC software. We used this spectrometer in the mid-IR range of  $400\text{--}4000\ \text{cm}^{-1}$ .

Dilatometry analyses were carrying out with a horizontal dilatometer 402PC NETZSCH. This technique is for the measurement of expansion or shrinkage during a controlled temperature/time program. We used alumina sample holder and push-rod, and air atmosphere in the kiln. Sample of powder compacts were preliminary pressed into cylinder of  $3\ \text{mm}$  diameter and controlled length. Temperature range was  $25\text{--}1200^\circ\text{C}$  with  $5^\circ\text{C}/\text{min}$  for heating and cooling rates.

## 3. Results

The XRD patterns for samples are given in Fig. 1 (a–c), for kaolinite (Kga-1) and for kaolinite–urea. Fig. 1a displays the common basal [001] distance of kaolinite of  $7.2\ \text{\AA}$ , and in Fig. 1b and c for intercalation complexes, a new peak appears with a  $d$  value of  $10.7\ \text{\AA}$ . It demonstrates that inter-layers contain some guest molecules leading to the expansion of the basal spacing of kaolinite by intercalation. The relative intensity of the  $7.2\ \text{\AA}$  peak indicates that intercalation is not fully completed. To compare the two processing methods, the intercalation ratios were obtained from peak heights [6]. They attain 69% from mixing and 75% from ball-milling techniques. The FWHM value of the  $10.7\ \text{\AA}$  peak is broader for the mechanochemical intercalation (Fig. 1b) than for intercalation by the aqueous suspension [9]. It is related to the increase of the structural disorder and the reduction of crystallite size during the intense mechanochemical grinding.

The reduction of intensity of non-basal peaks is also due to urea intercalation causing disorder in kaolinite stacking [21]. XRD of Fig. 1b and c also show that the second basal reflection of kaolinite is superposed with the third basal reflection of the urea-intercalated complex.

The significant expansion of basal distance of kaolinite is accompanied by a significant change in kaolinite surface properties. Intercalation process is firstly explained by a diffusion process within layers. Then existing hydrogen bonds between kaolinite outer hydroxyl groups and O of the adjacent silica layer are broken, and new hydrogen bonds through their respective H and O atoms with the O atom of tetrahedral sheets and H atom of octahedral sheets [22].

Infrared studies were performed with the urea–kaolinite complex to observe any changes at kaolinite interlayers. Experiment of pure kaolinite in Fig. 2a and b shows IR absorption bands commonly observed with well-ordered kaolinite. In the high wavenumber region, OH stretching bands are observed at  $3695$ ,  $3670$ ,  $3652$  and  $3620\ \text{cm}^{-1}$  [23]. They correspond to the inner OH stretching ( $3620\ \text{cm}^{-1}$ ), to the anti-phase stretching of inner-surface OH groups ( $3670$ ,  $3652\ \text{cm}^{-1}$ ) and to in-phase stretching of the three inner-surface OH groups ( $3695\ \text{cm}^{-1}$ ) [24].

In the lower wavenumber region, bands at  $1032$  and  $1009\ \text{cm}^{-1}$  are anti-symmetric stretching Si–O–Si vibrations. Beside, bands at  $1114$  and  $1102\ \text{cm}^{-1}$  are from symmetric stretching of outer Si–O

**Table 1**  
Chemical composition of Kga-1b kaolin (wt%) [19].

SiO <sub>2</sub>	Al <sub>2</sub> O <sub>3</sub>	TiO <sub>2</sub>	Fe <sub>2</sub> O <sub>3</sub>	FeO	MnO	MgO	Na <sub>2</sub> O	K <sub>2</sub> O	F	P <sub>2</sub> O <sub>5</sub>
44.2	39.7	1.39	0.13	0.08	0.002	0.002	0.013	0.05	0.013	0.034

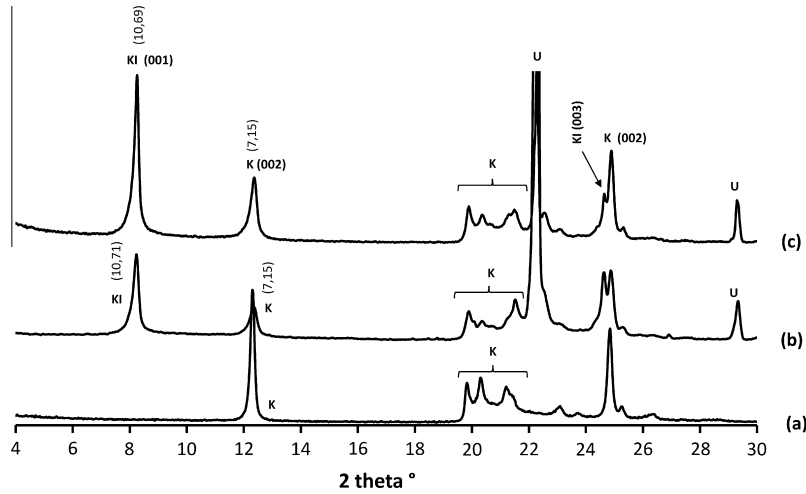


**Fig. 1.** XRD patterns of (a) kaolinite (b) kaolinite intercalated by ball milling method (c) kaolinite intercalated by mixing method. U: urea, K: kaolinite, KI: kaolinite intercalated.

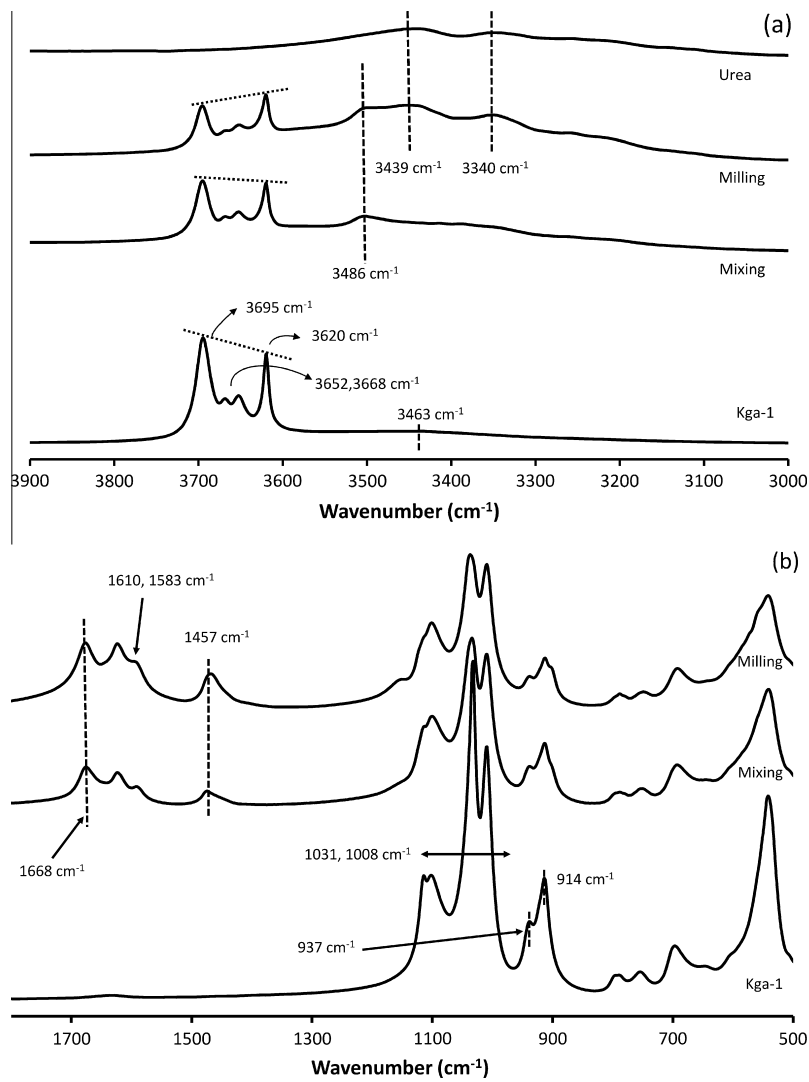


**Fig. 2.** FTIR spectrum of kaolinite original (Kga-1), intercalated kaolinite by ball milling and mixing methods. (a): High wavenumber region; (b): low wavenumber region.

bonds. In the 950–900  $\text{cm}^{-1}$  region a contribution of the bending of OH linked to  $\text{Al}^{3+}$  is found at 937 and 914  $\text{cm}^{-1}$  [3].

Additional broad bands of kaolinite at 1663 and 3436  $\text{cm}^{-1}$  are attributed to respectively bending and stretching modes of H–O–H on external surfaces [9].

On IR curves from kaolinite–urea obtained by mixing and ball milling, some typical bands of urea are distinguished. Particularly, bands at 1594  $\text{cm}^{-1}$  and 1619  $\text{cm}^{-1}$  are from N–H bending. The band at 1682  $\text{cm}^{-1}$  is assigned to both C=O stretching and  $\text{NH}_2$  bending. Finally, the band at 3261  $\text{cm}^{-1}$  is a combination of  $\text{NH}_2$  vibrations in urea.

For intercalated kaolinite, hydroxyl stretching bands at 3695, 3670, 3652 and 3620  $\text{cm}^{-1}$ , for inner-surface hydroxyls have unchanged positions. However, the absorption bands at 3695, 3670 and 3652  $\text{cm}^{-1}$  from inner-surface hydroxyls of kaolinite become weaker.

Differences occur between the two intercalation techniques, mixing and ball-milling, as the relative amplitude of 3695  $\text{cm}^{-1}$  band against that of 3620  $\text{cm}^{-1}$  is obviously reduced from original kaolinite to mixed and ball milled kaolinites. Since hydrogen's atoms of inner-surface hydroxyls are oriented towards the inter-layer, band difference evidences that weak hydrogen bonds can be formed between urea molecules and the inner-surface hydroxyls of kaolinite, but not with the inner-hydroxyls.

Differences also appear in the 3600–3000  $\text{cm}^{-1}$  region, since new bands appear at 3498, 3452 and 3351  $\text{cm}^{-1}$ . They are related to NH groups of urea, linked to kaolinite by hydrogen bonding. However, band amplitudes are higher with ball milling that is related to a larger availability of active sites for urea bonding. It is originated from the intensive mechanical treatment that leads to the weakening of kaolinite crystallinity [9]. For both intercalation processes, the principal mechanism of urea bonding is proposed in [21]. Hydrogen bonds are formed between oxygen atoms of the silica surface of kaolinite and the  $\text{NH}_2$  group of urea molecules.

Used thermal analyses are differential scanning calorimetry (DSC) and thermogravimetric analysis (TG) [25,26]. Thermal analyses against temperature were carried out under air and results are given in Fig. 3 for DSC, Fig. 4 for TG and Fig. 5 for DTG. For kaolin, successive curves stages are observed when temperature increases: – kaolinite dehydroxylation between 470 and 620 °C with a peak mass loss at 555 °C; – structural reorganization of dehydroxylated kaolinite between 980 and 1020 °C with no mass loss [27].

For intercalated kaolin the transformations are complex and correlation between DSC, TG and DTG curves may lead to the iden-

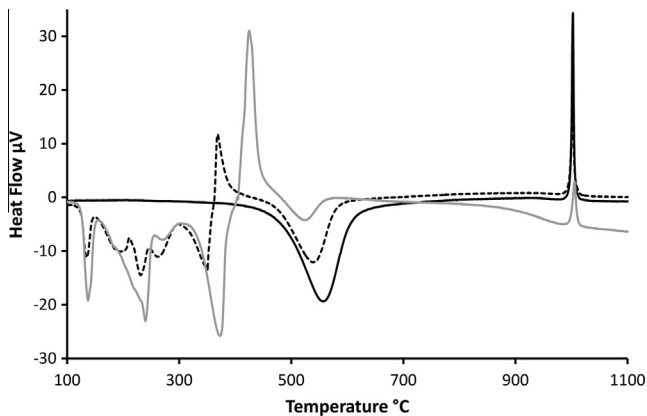


Fig. 3. Thermo analyses DSC of original kaolinite and of the two kaolinite–urea complexes. Kga-1: black line; mixing method: dashed line; milling method: grey line.

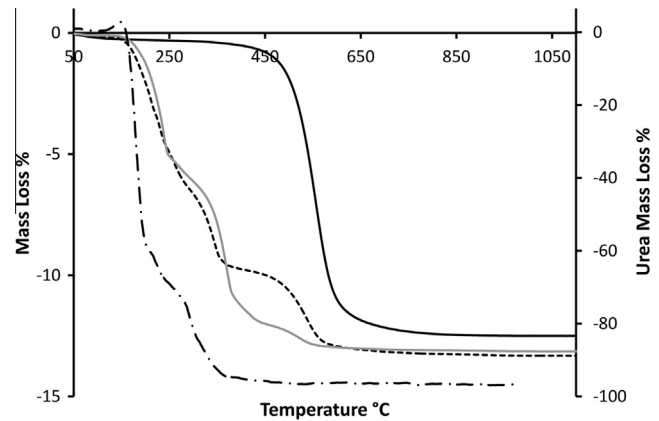


Fig. 4. Thermogravimetry of urea, original kaolinite, and of the two kaolinite–urea complexes. Kga-1: black line; mixing method: dashed line; milling method: grey line; urea: mixed line.

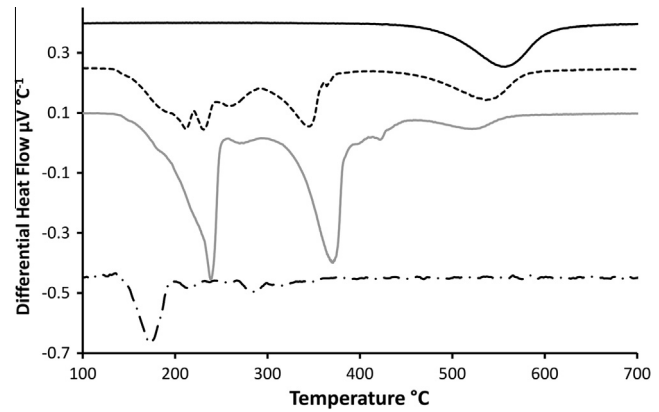


Fig. 5. Differential thermogravimetry of urea, original kaolinite, and of the two kaolinite–urea complexes. Kga-1: black line; mixing method: dashed line; milling method: grey line; urea: mixed line.

tification of transformations. The removal of moisture is observed in DSC at 134–136 °C correlated with a small mass loss. It is followed by endothermic transformations at 228 and 263 °C for mixed kaolin and at 238 °C for milled kaolin. On DTG, it is correlated with mass losses at 209 °C, 229 °C and 258 °C for mixed kaolin and at 238 °C for milled kaolin.

At 343 °C and 369 °C, strong endotherms are seen for mixed and milled kaolins that are correlated with significant mass losses on TG and DTG at 345 °C and 373 °C. Above, strong exotherms are at 373 °C and 425 °C, with small mass losses seen on DTG curves. It is followed by endotherms correlated with mass losses, which peak maximums are at 536 °C and 523 °C for mixed and milled kaolins.

In Fig. 3, exothermic peaks are at 990–1010 °C. With kaolin, the intensity of the exothermic peaks is high and with intercalated kaolin we observe the reduction of peak intensity, simultaneously to the increase of peak widths, whereas temperature at peak maximum are similar ( $1002 \pm 2$  °C).

In Fig. 6 we present the results of thermomechanical analyses of sintering densification against time and temperature, up to 1200 °C for the initial kaolinite and for the intercalated samples. Below 300 °C, the powder compact of kaolinite undergo a volume expansion due to thermal dilatation of phases without any physico-chemical changes. It is different with intercalated kaolinite since a slight and transitory volume expansion occurs due to the escape of gas from the thermal transformation of excess urea. It is well correlated with mass loss on TG curves in the same temperature range.

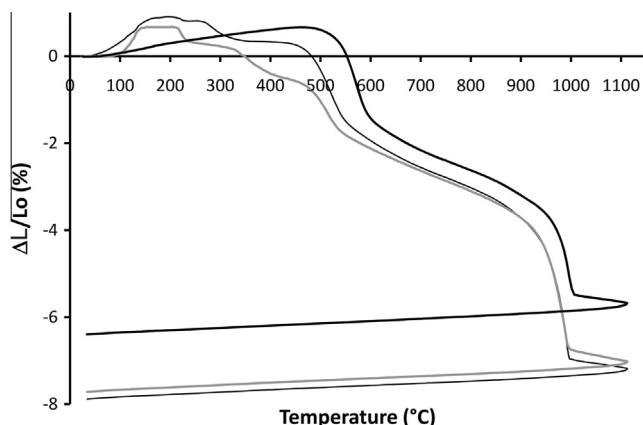


**Fig. 6.** Thermomechanical curves of Kga1 and of intercalated kaolinite with urea by mixing technique.  $\Delta L/L_0$  is the linear variation of sample during sintering. Kga-1: black line; mixing method: dashed line; milling method: grey line.

At about 300–400 °C, a first densification for mixed and milled kaolinite is observed from the early dehydroxylation of the intercalated phase. At higher temperature, shrinkage continues due the dehydroxylation of non-intercalated kaolinite, which takes place at temperature of 450 °C and up to 570 °C. Once again, TG curves show weight losses in the same temperature range. The main point is the shift to lower temperature of densification due to dehydroxylation from kaolinite to intercalated kaolinite that is about 50 °C for mixed kaolinite and about 70 °C for milled kaolinite.

Above 600 °C, shrinkage continues up to 970 °C that is related to densification of the structurally low ordered metakaolinite having a high specific surface and reactivity. At about 970–1000 °C, we observe an abrupt and extended shrinkage caused by the onset of the structural reorganization process of the quasi-amorphous metakaolinite. Curves of Fig. 6 evidence a  $\sim 25$  °C temperature shift that leads to a more important densification at a lower temperature.

Finally, densification is slow down at about 1008 °C for kaolinite and 990 °C for intercalated kaolinite.

During that sintering stage, two competitive processes occur: – a densification process of a highly reactive silico-aluminate phase with the progressive removal of porosity; – a strong recrystallization process inside the low ordered silico-aluminate phase, limiting the extend of densification.

For the ceramic paste containing Kga1 kaolin, quartz and alkaline feldspar (Fig. 7), the sintering process is also separated into

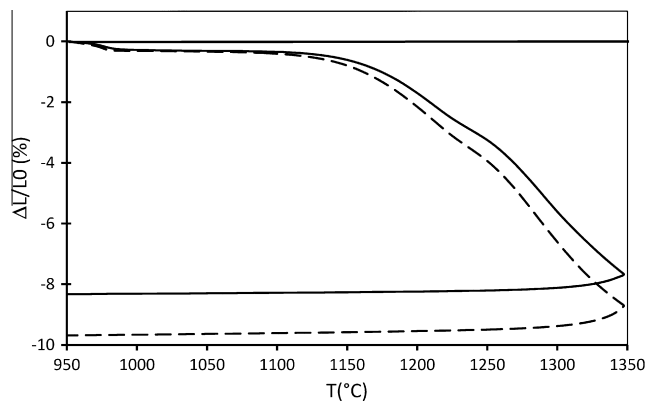


**Fig. 7.** Thermomechanical curves of the vitrified ceramic paste containing Kga1 kaolin, quartz and alkaline feldspar.  $\Delta L/L_0$  is the linear variation of sample during sintering. Non-intercalated Kga-1: black line; intercalated Kga-1: dashed line.

successive steps with temperature. Below 950 °C, we see very similar thermal transformations of pastes with kaolin and intercalated kaolin because temperature is relatively low and only individual thermal transformations occur. Consequently, only the comparison of curves is plotted above 950 °C, to examine the intercalation role on densification of the ceramic paste. Fig. 7 evidences the role of intercalated kaolinite, since it reduces the sintering temperature for a similar densification. Temperature difference increases with temperature, attaining 30 °C at 1300 °C.

#### 4. Discussion

From DRX curves of Fig. 1 the new peak value at 10.7 Å is related to intercalated kaolinite phase. The relative intensity of this peak against the 7.2 Å peak reveal the high intercalation degree whereas the simple method used by mixing or short time ball milling. However differences occur between the two methods that are related to the role of the intensive energy of grinding. It leads to increase the density of disorder in kaolinite lattice and layer stacking that is evidenced by the larger peak width of intercalated kaolinite with urea by grinding [28]. Beside, a more structurally disordered kaolinite is favorable to the increase of adsorption density of urea, which is observed with a higher intercalation ratio of 75% from ball-milling.

For the IR results, the variation of band intensities supports the intercalation model proposed by White [11]. It shows that hydrogen bonds are formed through the NH<sub>2</sub> groups of urea on the silicate network on kaolinite surface [29]. It concludes on the effective intercalation of urea.

Different thermal behavior of kaolin and intercalated kaolin evidences the complex mechanisms occurring during the structural reorganization above 950 °C. At 1002 ± 2 °C, exotherms are associated with the onset of the formation of a new spinel phase that will be more or less rapidly transformed into mullite at higher temperature.

Kga-1 kaolinite, have a whole structural reorganization (950–1300 °C) that follows the typical transformation path from metakaolinite to spinel phase (Si<sub>2</sub>Al<sub>2</sub>O<sub>4</sub>) and then to mullite (Si<sub>2</sub>Al<sub>6</sub>O<sub>13</sub>), that is extensively described in the literature [30]. Above 1100 °C, literature results evidence the continuous nucleation and growth of mullite and the progressive disappearance of spinel phase. However, DSC–TG results evidence that intercalated kaolinite has a different behavior. It is suggested that intercalated kaolinite behaves similarly to kaolinite having low crystallinity degree. Intercalation induces the reduction of DSC exotherm at  $\sim 1000$  °C (Fig. 3) that is similar to that obtained when Kga-1 having a high crystallinity degree is replaced by Kga-2 kaolin having a low crystallinity degree [31]. In general, when crystallinity degree decreases, both mullite size and number density of crystallites are increased at the same temperatures.

It was also studied the role of kaolinite heating rate [32] on thermal transformation, and in this study, it is shown that it is also representative of differences between kaolinite and intercalated kaolinite. It was proved that fast heating rate favors the formation of a more disordered metakaolinite phase that accelerate the overall thermal processes above 1000 °C. Particularly, sintering is accelerated together with mullite recrystallization through a more direct transformation path that limits the occurrence of the intermediate spinel phase [33].

Above 650 °C, dehydroxylated kaolinite (metakaolinite) is almost amorphous, though the dehydroxylation process is topotactic and the particles retain the pseudohexagonal morphology.

With urea, TG data indicate that successive structural modifications occur during the destruction of the kaolinite–urea complex. As for other kaolinite–intercalated species, desorption leads to

continuous changes of either the basal spacing and of the way to return to structurally ordered complexes.

The reduction of dehydroxylation temperature is explained by the increase of the interlayer space leading to the weakening of interlayer hydrogen bonds. Simultaneously, dehydroxylation reveal the progressive ordering in stacking of kaolinite layers that is highlighted by studies of IR and XRD spectra after heat treatment [34]. However the number of layers in diffracting domains notably decreases as a consequence of the intercalation process. In general, structural characteristics of dehydroxylated kaolinite are changed by intercalation in accordance with the reported trend in different kaolinites [35] and having a different degree of stacking ordering [36,37]. Consequently, the sequence and kinetic of further phase transformations depends on the structural arrangement of metakaolinite. It is extensively reported in the literature, showing that the conversion path to mullite depends strongly on the structural characteristics and type of homogeneity at low scale [38]. As an example, the mechanical activation of kaolinite–alumina mixtures results in the decrease of activation energy values for mullite formation [39]. In a same way, the decomposition of metakaolinite to mullite as a function of the degree of structural order of the starting kaolinite was also investigated. It was found that the activation energy for mullite nucleation and growth is related to the defective structure of the starting kaolinite [40].

For temperatures above 1000 °C, competitive processes of densification and recrystallization occur. Densification extend is related to kaolinite crystallite size and structural arrangement. Intercalated kaolinite behaves similarly to delaminated kaolinite by intensive grinding, and the specific surface is significantly increased [41,42]. It increases the inter-particle reactivity that reduces the sintering temperature, accelerates the densification rate, and reduces the phase transformation temperature [43,44].

Changes in recrystallization processes are obtained when the structural order of metakaolinite is changed. Literature extensively reports the role of the heating rate, which change the mechanism of nucleation and growth of nuclei of spinel and mullite [32,45,46]. It results from the shift of diffusion limited growth to the rate of nucleation surface controlled with increasing heating rate. The apparent activation energy of spinel phase crystallization decreases if heating rate increases [33,47,48].

Finally, sintering of the ceramic paste is also changed when intercalated kaolinite is used. At 980–1000 °C, the densification process occurs simultaneously with the onset of kaolinite structural reorganization process. Above 1100 °C, the alkaline feldspar starts to form a glassy phase, inducing a liquid phase sintering process [20]. As temperature increases, liquid reacts with the high temperature form of kaolinite and quartz to form a dense ceramic. The liquid phase sintering enhances the formation of mullite since diffusion processes of species are enhanced.

Another interesting point is that sintering densification of the ceramic paste is also enhanced whereas the successive stages of ceramic processes during which mixtures are obtained by wet ball milling during 2 h. It evidences that whereas the wet ball milling, the form of exfoliated kaolinite is maintained [49]. Obtaining a highly reactive kaolin becomes relatively simple in comparison to kaolin from delamination by grinding. Beside, intercalation proved to maintain morphological characteristics comparable to that of the initial kaolinite.

## 5. Conclusion

The thermal transformations of intercalated kaolin with urea occur with several mechanisms depending on temperature. XRD and IR studies evidence the effectiveness of urea intercalation and bonding in interlayers. Whereas the simple intercalation

methods by aqueous mixing and ball milling, the intercalation degree attains 72% and 69% respectively. This point is very important, supporting that high intercalation degree of kaolinite mineral can be attained in industrial processes using kaolin or kaolinitic clays.

Obtained results by IR, DSC and TG methods as by thermomechanical studies provide complementary details on structural and physical transformation when intercalated kaolin is heated. At expanded interlayers, bonds are formed between inner-surface hydroxyls of kaolinite and NH groups of urea that contribute to obtain physical properties of intercalated kaolinite similar to that of delaminated kaolinite by intensive grinding.

From thermal analyses, successive structural modifications with temperature and particularly, the reduction of dehydroxylation temperature is determinant in temperatures and kinetics of structural transformations and in rate of sintering densification. Above 1000 °C, it induces changes in the relative importance of competitive processes of densification and recrystallization. Intercalated kaolinite behaves similarly to delaminated kaolinite by intensive grinding that reduces the sintering temperature of more than 25 °C, accelerating the densification rate. Such temperature shift is sufficient to induce a significant reduction of the specific energy consumption during large scale manufacturing of clay ceramics for building.

## References

- [1] Fédération Française des tuiles et briques (FFTB), 2014. <<http://www.fftb.org/tbffin00.htm>>.
- [2] Junxia Peng, Yubo Zhao, Lihua Jiao, Weimin Zheng, Lu Zeng, CO<sub>2</sub> emission calculation and reduction options in ceramic tile manufacture, *Foshan Case Energy Proc.* 16 (2012) 467–476.
- [3] H. Cheng, Q. Liu, J. Yang, X. Du, R.L. Frost, The thermal behavior of kaolinite intercalation complexes—a review, *Thermochim. Acta* 545 (2012) 1–13.
- [4] H. Cheng, Q. Liu, J. Yang, X. Du, R.L. Frost, Influencing factors on kaolinite–potassium acetate intercalation complexes, *Appl. Clay Sci.* 2010 (50) (2010) 476–480.
- [5] R.L. Frost, J. Kristof, L. Rintoul, T.J. Kloprogge, Raman spectroscopy of urea and urea-intercalated kaolinites at 77 K, *Spectrochim. Acta A* (1999) 1681–1691.
- [6] A. Kalendova, J. Zykova, V. Matejka, M. Machovsky, J. Malac, PVC inorganic hybrids based on kaolinite/urea intercalates, in: *The Fifth International Conference on Quantum, Nano and Micro Technologies*, 2011, pp. 109–113.
- [7] M. Trevino, J.C. Coles, Kaolinite properties, structure and influence of metal retention on pH, *Appl. Clay Sci.* 23 (2003) 133–139.
- [8] K.P. Nicolini, C.R. Fukamachi, F. Wypych, A.S. Mangrich, Dehydrated halloysite intercalated mechanochemically with urea: thermal behavior and structural aspects, *J. Colloid Interface Sci.* 338 (2009) 474–479.
- [9] E. Mako, J. Kristof, E. Horvath, V. Vagvolgyi, Kaolinite–urea complexes obtained by mechanochemical and aqueous suspension techniques—a comparative study, *J. Colloid Interface Sci.* 330 (2009) 367–373.
- [10] M. Valaskova, M. Rieder, V. Matejka, P. Capkova, A. Sliva, Exfoliation/delamination of kaolinite by low-temperature washing of kaolinite–urea intercalates, *Appl. Clay Sci.* 35 (2006) 108–118.
- [11] R.L. Ledoux, J.L. White, Infrared studies of hydrogen bonding interaction between kaolinite surfaces and intercalated potassium acetate, hydrazine, formamide, and urea, *J. Colloid Interface Sci.* 1966 (21) (1966) 127.
- [12] J. Kristof, R.L. Frost, E. Horvath, L. Kocsis, J. Inczedy, Thermoanalytical investigations on intercalated kaolinites, *J. Therm. Anal.* 53 (1998) 467–475.
- [13] D.L. Smith, M.H. Milford, J.J. Zuckerman, Mechanism for intercalation of kaolinite by alkali acetates, *Science* 153 (1966) 741–743.
- [14] G.J. Churchman, J.S. Whitton, G.G.C. Claridge, B.K.G. Theng, Intercalation method using formamide for differentiating halloysite from kaolinite, *Clays Clay Miner.* 32 (1984) 241–248.
- [15] B.K.G. Theng, G.J. Churchman, J.S. Whitton, G.G.C. Claridge, Comparison of intercalation methods for differentiating halloysite from kaolinite, *Clays Clay Miner.* 32 (1984) 249–258.
- [16] F. Franco, M.D. Ruiz Cruz, Factors influencing the intercalation degree ('reactivity') of kaolin minerals with potassium acetate, formamide, dimethyl sulphoxide and hydrazine, in: *Clay Miner.* 39 (2004) 193–205.
- [17] A. Weiss, A secret of Chinese porcelain manufacture, *Angew. Chem. Int. Ed. Engl.* 2 (1963) 697–703.
- [18] S. Yariv, H. Cross, Introduction to Organo-Clay Complexes and Intercalations, Marcel Dekker, New York, 2002, pp. 39–111.
- [19] R.J. Pruett, H.L. Webb, Sampling and analysis of Kga-1 B well-crystallized kaolin source clay, *Clays Clay Miner.* 41 (1993) 514–519.
- [20] F.H. Norton, *Fine Ceramics: Technology and Applications*, McGraw-Hill, 1978. ISBN-13: 978-0882755823.

- [21] Qinfu Liu, Shuai Zhang, Hongfei Cheng, Ding Wang, Xiaoguang Li, Xinjuan Hou, Thermal behavior of kaolinite–urea intercalation complex and molecular dynamics simulation for urea molecule orientation, *J. Therm. Anal. Calorim.* 117 (2014) 189–196.
- [22] S. Olejnik, A.M. Posner, J.P. Quirk, The intercalation of polar organic compound into kaolinite, *Clay Miner.* 8 (1970) 241–434.
- [23] R.L. Ledoux, J.L. White, Infrared studies of hydrogen bonding interaction between kaolinite surfaces and intercalated potassium acetate, hydrazine, formamide, and urea, *J. Colloid Interface Sci.* 21 (1966) 127–152.
- [24] E. Balan, A. Marco Saitta, F. Mauri, C. Calas, First-principles modeling of the infrared spectrum of kaolinite, *Am. Mineral.* 86 (2001) 1321–1330.
- [25] R.M. Barrer, Shape selective sorbents based on clay minerals—a review, *Clays Clay Miner.* 37 (1989) 385–605.
- [26] A.L. Kuzniarowa, *A Thermal Analysis of Organo-Clay Complexes*, Marcel Dekker, New York, 2002, pp. 273–344.
- [27] U. Shuali, M. Steinberg, S. Yariv, M.M. Vonmos, G. Kahr, A. Rub, Thermal analysis of sepiolite and palygorskite treated with butylamine, *Clay Miner.* 25 (1990) 107–119.
- [28] P. Aparicio, E. Galan, R.E. Ferrell, A new kaolinite order index based on XRD profile fitting, *Clay Miner.* 41 (2006) 811–817.
- [29] R.L. Ledoux, J.L. White, Infrared studies of hydroxyl groups in intercalated kaolinite complexes, *Clays Clay Miner.* 13 (1965) 289–315.
- [30] K. Traore, F. Gridi-Bennadji, P. Blanchart, Significance of kinetic theories on the recrystallization of kaolinite, *Thermochim. Acta* 451 (2006) 99–104.
- [31] O. Castelein, R. Guinebretière, J.P. Bonnet, P. Blanchart, Shape, size and composition of mullite nanocrystals from a rapidly sintered kaolin, *J. Eur. Ceram. Soc.* 21 (2001) 2369–2376.
- [32] O. Castelein, B. Soulestin, J.P. Bonnet, P. Blanchart, The influence of heating rate on the thermal behaviour and mullite formation from a kaolin raw material, *Ceram. Int.* 27 (2001) 517–522.
- [33] P. Ptáček, F. Šoukal, T. Opravil, M. Nosková, J. Havlica, J. Brandštetr, The kinetics of Al–Si spinel phase crystallization from calcined kaolin, *J. Solid State Chem.* 183 (2010) 2565–2569.
- [34] Hongfei Cheng, Qinfu Liu, Jing Yang, Songjiang Ma, Ray L. Frost, The thermal behavior of kaolinite intercalation complexes—a review, *Thermochim. Acta* 545 (2012) 1–13.
- [35] M. Bellotto, A. Gualtieri, G. Artioli, S.M. Clark, Kinetic study of the kaolinite–mullite reaction sequence. Part I: kaolinite dehydroxylation, *Phys. Chem. Miner.* 22 (1995) 207–214.
- [36] R.C. Mackenzie, Simple phyllosilicates based on gibbsite- and brucite-like sheets, in: R.C. Mackenzie (Ed.), *Differential Thermal Analysis*, Academic Press, London, 1970. 498–37.
- [37] J.G. Cabrera, M. Eddleston, Kinetics of dehydroxylation and evaluation of the crystallinity of kaolinite, *Thermochim. Acta* 70 (1983) 237–247.
- [38] K. Okada, N. Otsuka, Characterization of the spinel phase from SiO<sub>2</sub>–Al<sub>2</sub>O<sub>3</sub> xerogels and the formation process of mullite, *J. Am. Ceram. Soc.* 69 (1986) 652–656.
- [39] E. Elmas, K. Yildiz, N. Toplan, H. Özkan Toplan, The non-isothermal kinetics of mullite formation in mechanically activated kaolinite–alumina ceramic system, *J. Therm. Anal. Calorim.* 108 (2012) 1201–1206.
- [40] A. Gualtieri, M. Bellotto, G. Artioli, S.M. Clark, Kinetic study of the kaolinite–mullite reaction sequence. Part II: mullite formation, *Phys. Chem. Miner.* 4 (1995) 215–222.
- [41] E. Makó, J. Kristóf, E. Horváth, V. Vágvölgyi, Kaolinite–urea complexes obtained by mechanochemical and aqueous suspension techniques—a comparative study, *J. Colloid Interface Sci.* 330 (2009) 367–373.
- [42] Kinue Tsunematsu, Hiroshi Tateyama, Satoshi Nishimura, Kazuhiko Jinnai, Delamination of kaolinite by intercalation of urea, *J. Ceram. Soc. Jpn.* 100 (1992) 178–181.
- [43] J. Ondruška, T. Keppert, I. Medved, L. Vozár, Isothermal dilatometric study of sintering in kaolin, *Int. J. Thermophys.* 35 (2014) 1946–1956.
- [44] E. Kamseu, A. Rizzuti, P. Miselli, P. Veronesi, C. Leonelli, Use of noncontact dilatometry for the assessment of the sintering kinetics during mullitization of three kaolinitic clays from Cameroon, *J. Therm. Anal. Calorim.* 98 (2009) 757–763.
- [45] J.A. Pask, A.P. Tomsia, Formation of mullite from sol–gel mixtures and kaolinite, *J. Am. Ceram. Soc.* 74 (1991) 2367–2373.
- [46] A.K. Chakraborty, DTA study of preheated kaolinite in the mullite formation region, *Thermochim. Acta* 398 (2003) 203–209.
- [47] P. Ptáček, F. Šoukal, T. Opravil, J. Havlica, J. Brandštetr, Crystallization of spinel phase from metakaoline: the nonisothermal thermodilatometric CRH study, *Powder Technol.* 243 (2013) 40–45.
- [48] K. Boussois, N. Tessier-Doyen, P. Blanchart, Anisotropic kinetic of the kaolinite to mullite reaction sequence in multilayer ceramics, *J. Eur. Ceram. Soc.* 33 (2013) 243–249.
- [49] M. Valášková, M. Rieder, V. Matějka, P. Čapková, A. Slíva, Exfoliation/delamination of kaolinite by low-temperature washing of kaolinite–urea intercalates, *Appl. Clay Sci.* 35 (2007) 108–118.